JOURNAL GEOLOGICAL SOCIETY OF INDIA
Vol.89, April 2017, pp.363-368

Modeling of Source Parameters of the 15 December 2015 Deogarh Earthquake of M_w 4.0

Prantik Mandal*, B. Singh, P. Nagendra and A.K. Gupta
CSIR- National Geophysical Research Institute, Uppal Road, Hyderabad – 500 007, India. ***E-mail:** *prantik@ngri.res.in*

ABSTRACT

We herein present source parameters and focal mechanism of a rare cratonic upper crustal earthquake of M_w4.0, which occurred at 8 km depth (centroid depth) below a region near Deogarh, Jharkhand. For our study, we used broadband waveform data from a seismic network of 15 three-component seismographs in the eastern Indian craton. The average seismic moment, moment magnitude and source radius are estimated to be 1.1 x 10^{15} N-m, 4.0 and 180.6 m, respectively. The high average stress drop of 14.27 MPa could be attributed to its lower-crustal origin. The mean corner frequency is calculated to be 4.1 Hz. To study the source mechanism, we perform a deviatoric constrained full waveform moment tensor inversion of multiple point sources on the band-passed (0.06 - 0.14 Hz) broadband displacement data of the Deogarh event, using ISOLA software. The best fit is obtained for the source at 8 km centroid depth, with a moment magnitude 3.7, and a right-lateral strike-slip mechanism with strike 162º, dip 72º and rake 169º. The P-axis orients N24ºE, which is parallel to the direction of the absolute plate motion direction of Indian plate, while T-axis orients E-W, which is parallel to the strike of the pre-existing Damodar Graben (DG) of Gondwana age. The occurrence of this earthquake is attributed to the neotectonic reactivation of a fault associated with the E-W trending DG shear zone.

INTRODUCTION

A M_w4.0 earthquake occurred in the lower crust (at 8 km centroid depth) on 15 December 2015 at 02:35:16.8 GMT. The epicenter of this earthquake (24.034ºN, 86.649ºE, Fig. 1) was within the Damodar graben (DG) in the Chotanagpur granitic gneissic terrain (CGGT) of the eastern Indian craton, which is known for its low seismic activity. This region is delimited by the lower Himalayan on the northern side while the Singhbhum craton bounds it to the south. The Bay of Bengal lies to the east of it while the Central Indian tectonic zone (CITZ) is to the west. Available focal mechanism data suggests dominating strike slip deformation in this region (Khan et al., 2011). This is further supported by the results of moment tensor inversion modeling of two smaller earthquakes of M3.0, which has also shown strike-slip behavior (Kayal et al., 2009). This earthquake was perceived at distances of 100 km as evidenced by felt reports but only resulted in minor damage due to its location and depth. This earthquake was recorded at 9 out of 15 three-component broadband stations in a seismic network operated by the National Geophysical Research Institute, Hyderabad, India, in the eastern Indian shield (Fig. 2). This data set enables us to study the source characteristics of this earthquake; through inversion modeling for source parameters and moment tensors the results of which are presented in this paper. An attempt has also been made to infer about the causative source process involved in generating this lower-crustal cratonic event.

SEISMICITY IN THE STUDY AREA

Small to moderate size earthquakes have been occurring in some parts of the eastern Indian craton (Gupta et al., 2014). Two historical damaging earthquakes (viz. 31 July 1868 M4.3 Hazaribagh and 30 September 1868 M5.7 Manbhum) have occurred in the Chotanagpur plateau (Fig. 1; Oldham, 1883). Another significant historical earthquake of M5.2 also took place on 8 May 1963, in the Singhbhum shear zone (Fig. 1; USGS). In 1964, three moderate size (ML: 5.3-5.5) earthquakes occurred in the Midnapur district of West Bengal (Chandra, 1977). The fault plane solutions of these three earthquakes revealed a strike-slip motion along a preferred ENE -WSW trending fault plane with an N-S oriented maximum compression (Fig. 1). In 1995, two moderate earthquakes of ML 5.0 took place in the Bonaigarh region near the EGMB (Eastern Ghat Mobile Belt)-Singhbhum craton contact zone (Gupta et al., 2014). Available historical seismicity data suggest that this area had also experienced two or more earthquakes of ML 5.2 in 1958 and 1962 (Fig. 1), respectively, and two earthquakes of magnitudes ML 4.4 and 4.1 occurred in January 1986 (Gupta et al. 2014). Also, one earthquake of ML 4.3 has also occurred in 1993 along the Sukhinda thrust (Fig. 1). Additionally, 26 smaller earthquakes (M<3.0) were reported by the Geological Survey of India (GSI) through a temporary microearthquake (MEQ) monitoring in the Bonaigarh-Talchir area during January to mid-May, 1997. Further, recently 160 smaller events, which have occurred in the Dhanbad, Jharkhand and its surroundings areas during 2007-08, were reported by the Indian School of Mines single station observatory (Khan et al., 2011). Moment tensor solutions of two local earthquakes of M<3.0, which occurred in the surrounding regions of Dhanbad, Jharkhand, suggested a left lateral strike-slip faulting at 26 km depth (Fig. 1; Kayal et al. 2009). Thus, we can infer from the above discussion that the strike-slip sense of motion is the dominant deformation mode in our study area.

SEISMIC NETWORK AND EARTHQUAKE DATA

With an objective to delineate the crust-mantle structure, CSIR-NGRI (Council of Scientific and Industrial Research-National Geophysical Research Institute), Hyderabad, India, has established a semi-permanent seismic network of 15 three-component broadband seismographs in the eastern Indian shield, in 2013 (Fig.1). This network has been established under the 12th five-year research project scheme of the CSIR-NGRI. Each seismograph station consists of a 24-bit Reftek recorder and a 120 s Reftek sensor, equipped with GPS time tagging. The seismograph record at 50 samples/s at a high gain. The stations are installed on the hard rock site resulting in a high signal to noise ratio (Fig. 2). Nine out of fifteen seismographs of the above network have recorded the 15 December 2015 Deogarh earthquake (Fig. 2; Table 1).

METHODOLOGY

Estimation of Hypocentral Parameters

Earthquake location for the 15 December 2015 Deogarh event (Fig. 1) is obtained through the location program inbuilt in SEISAN software (Havaskov and Ottemoller, 2003). For this purpose, arrival times of P- and S- waves from nine three-component seismograph

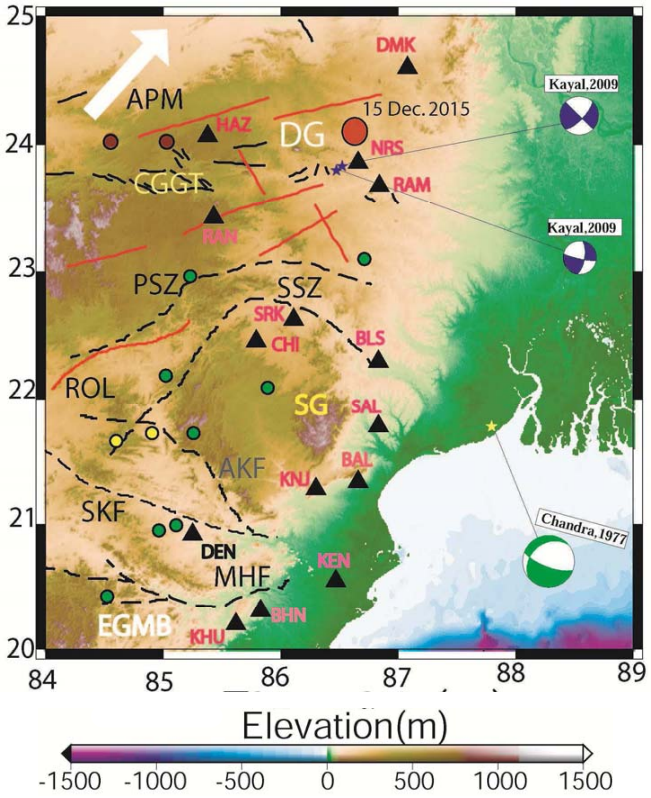

Fig.1. Three-component broadband seismograph stations (marked by solid black triangles) of the CSIR-NGRI, Hyderabad, superimposed on elevation map of Eastern Indian Shield. The big white arrow indicates the direction of absolute plate motion (APM) of the Indian plate as obtained from the NUVEL1A global plate model in a no rotation frame and with a fixed Eurasian plate, respectively (DeMets et al., 1990). SKF, AKF, MHF, ROL, SSZ and PSZ represent Sukinda thrust, Ankul fault, Mahanadi fault and Roulkela lineament, Singhbhum shear zone and Purulia shear zone, respectively. These major faults/shear zones are shown by black dotted lines. Lineaments are marked by solid red lines. DG, CGGT, EGMB and SG represent Damodar graben, Chotanagpur Granitic Gneissic Terrain, Eastern Ghats Mobile Belt and Singhbhum Granite, respectively. Small black solid lines within the DG mark fractures/ faults. A brown filled large circle marks the location of the 15 December 2015 Deogarh event. Solid brown circles mark two historical earthquakes (viz. 1968 M4.3 Hazaribagh and 1968 M5.7 Manbhum) while yellow solid circles mark two M5 events in 1863 and 1997, respectively. And solid green circles mark events of M3.0-4.9. The yellow and violet stars show locations of three local M4 events in CGGT and West Bengal, for which available focal mechanisms are also shown.

stations and the modified average one-dimensional crustal velocity model (Kayal et al., 2009) were used (Fig. 2). The velocity model consists of six layers, the tops of which are at 0.0, 4.0, 8.0, 12.0, 15.3, and 40.1 km, with P-wave velocities of 5.62, 5.72, 5.79, 5.87, 6.61, and 8.14 km/s, respectively. The distance between station and epicenters varies from 19.4 km to 438 km. This network resulted in an azimuthal gap of 123°. The average location rms is 0.55 s. The mean errors estimates in X-direction, Y-direction and Z-direction are 1.4, 1.9 and 1.5 km, respectively. Note that only three (DMK, NRS, & HAZ) out of nine broadband stations are having epicentral distances less than 100 km (Table 1). Therefore, data recorded at these three stations could be considered as local earthquake data whose P- and S-pick ups will be reliable. But, P- and S- pick ups for remaining six stations (at epicentral distances more than 100 km) would be doubtful.

Table 1. Location, elevation and epicentral distances for the nine broadband seismograph stations in the eastern Indian shield, which have recorded the 2015 Deogarh earthquake

Station	Latitude (°N)	Longitude (°E)	Elevation (km)	Eicentral distance (km)
NRS	23.86	86.66	0.217	19
RAM	23.55	70.47	0.200	36
DMK	24.60	87.08	0.199	76
HAZ	24.07	85.38	0.594	129
CHI	22.46	85.79	0.293	195
SAL	21.78	86.83	0.086	250
BLS	21.34	86.66	0.051	298
BHN	20.31	85.83	0.074	421
KHU	20.20	85.62	0.062	438

Further, all the stations are lying at distances, which are much more than the focal depth. Thus, S-pick ups at most of the stations (except NRS and DMK) would be doubtful. In this case, hypocentral depth estimate would be questionable, however, epicentral location would be quite reliable. Thus, to obtain a more robust focal depth a moment tensor inversion using the ISOLA software was performed. After locating the Deogarh event (Fig. 1), estimates of the source parameters and moment tensors using the methodologies as described in the following.

Estimation of Earthquake Source Parameters

An instrumental correction was applied to the broadband waveform data of the 15 December 2015 Deogarh earthquake, using pole-zero files of the sensor through the in-built "transfer" facility of SAC

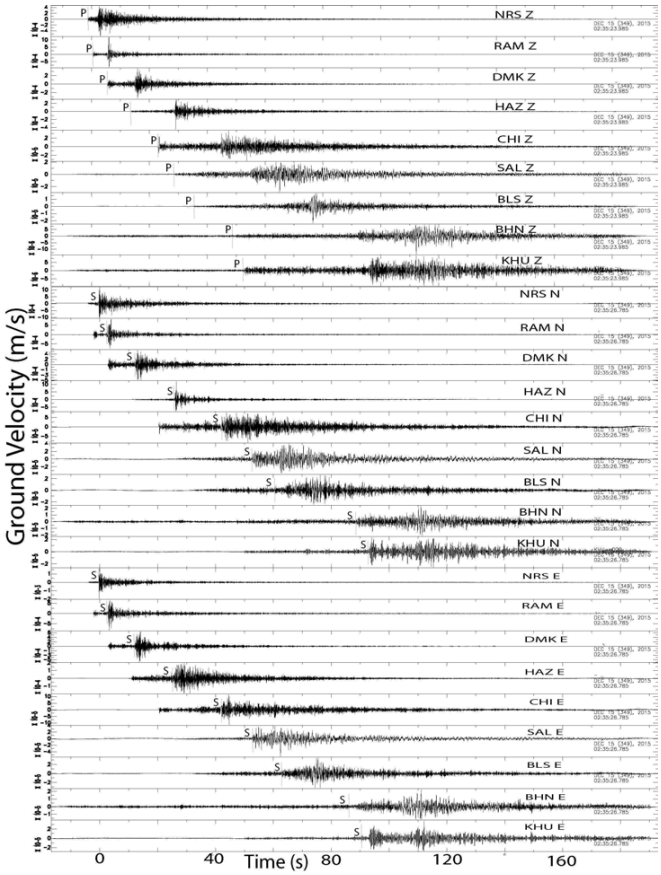

Fig.2. A plot showing 3-component broadband velocity waveforms for the 15 December 2015 Deogarh event recorded at nine seismograph stations in the eastern Indian craton. The P- and S-arrivals are marked by P- and S- on the different components of seismograms.

(Seismic Analysis Code), followed by the application of the functions "mean" and "trend removal" to our data, through SAC. A time window of 5.12 s was then selected beginning at the S-arrival from RTZ components. After obtaining the windowed S-wave data, a 5% cosine tapering on the both sides was applied. Finally, the S-wave spectra for the R, T and Z components using the in-built FFT (fast Fourier transform) facility of the SAC was computed. These S-wave spectra are used as the input data for the Levenberg–Marquardt inversion modeling to obtain the best fit spectra. In this inversion scheme, initial guesses for corner frequency (f_c) and long period spectral level (Π_o) are made from the respective spectra and the modeled spectra, i.e., the initial corner frequency is determined by matching the observed spectra and modeled spectra. After obtaining initial values, inversion modeling based on the ω-square source spectral model was performed to estimate the best-fit inverted spectra, by iteratively minimizing the normalized difference between inverted and observed spectra that provides the required model parameters, i.e., corner frequency and long-period spectral level values. Using these model parameters, other source parameters like source radius, static stress drop, seismic moment and moment magnitude was compute, using some well-known empirical relations.

We know that A_o, the source term for S-waves (high frequency fall-off (γ) = 2) can be written as (Boatwright, 1980):

$$A_0 = \Pi_0/[(1 + (f/f_c))^{2\gamma}]^{0.5} = \Pi_0/[(1 + (f/f_c))^4]^{0.5} = \Pi_0/B_4^{0.5} \quad (1)$$

From equation (1), we can write the spectral amplitudes at a distance R from the source, with no attenuation effect, as (Fletcher, 1995):

$$\ln A(f, R) = \ln[\Pi_0/[(1 + (f/f_c))^4]^{0.5}] - \ln R - \omega t^*/2 \quad (2)$$

where, $t^* = R/Q_o V_s$. Q_o is the quality factor while R is the hypocentral distance. Since, the formula for seismic moment is corrected from the geometrical spreading eûect, thus, the 'R' term can be dropped from equation (2). We now expand the B_4 term following the Taylor series as a Newton–Raphson's method to find roots of non-linear equations (Press et al. 1992), which yields the final equation as:

$$A(f) = \ln\Pi_0 - 0.5\ \ln B_4 + 2B_4^{-1}(f/f_c)^4\ (\Delta f_c/f_c) - \omega t^*/2 \quad (3)$$

We solve equation (3) using a least-squares algorithm to obtain the model parameters after 10 iterations. In fact, we minimize the error in least squares sense by solving:

$$D = GM \quad (4)$$

where, the model parameter matrix M, sensitivity matrix G and data matrix D are

$$\begin{aligned} M &= [\ln P_o,\ t^*,\ Df_c]^T \\ G &= [1,\ -\omega/2,\ 2B_4^{-1}(f/f_c)^4/f_c] \\ D &= [\ln A(f) + 0.5\ \ln B_4] \end{aligned} \quad (5)$$

Using Newton's method for quasi-linear equation

$$\Delta M = (G^T G)^{-1} G^T \Delta D \quad (6)$$

where, ΔM is the change in model parameters and ΔD is the difference between predicted data and observed data. The solution is found iteratively according to $M_k = M_o + M_{k-1}$ where M_o is the initial model. Since the sensitivity matrix tends to singular, we use the Lavenberg-Marquardt inversion technique to estimate $\ln\Pi_o$ and f_c with 10 iterations. Using this technique, equation (6) can be written as:

$$\Delta M = (G^T G + \lambda I)^{-1} G^T \Delta D \quad (7)$$

where, λ is the Levenberg–Marquardt adjustable damping parameter and I is the identity matrix.

In this inversion scheme, first we set the initial guessed value of Δf_c to 0.1 Hz for all events, while that of Π_o is selected visually from the respective low-frequency spectral level. And, the initial guessed value of t* is calculated using the equation $t^* = R/Q_o V_s$, where R is the hypocentral distance (in km). And for the Singhbhum region, Q_o considers to be 508 (Singh et al., 2004) while V_s assumes to be 3.5 km/s. Next, we estimate the normalized difference between the computed spectra obtained from the theoretical formula and that yielded from equation (1) at each iteration. The maximum difference is selected from the initial guessed values of Π_o, t* and f_c, and the minimum value is set based on the accuracy of the Π_o, t* and f_c values that one can expect to obtain from the inversion of noisy data (Mandal and Dutta, 2011). We also assign an initial value to λ, say 0.001. The change in model parameter vector (ΔM) is derived by substituting the initial guessed values into equation (7). In the next iterations, a new model parameter is computed according to $M_{r+1} = M_r + DM_r$, where M_r and DM_r are the model parameters and change in parameter values at the r^{th} iteration. Thus, after 10 integrations, we obtain the best fit model which provides the model parameters i.e. f_c, t* and Π_o. In this study, the final λ values, which provide the best fit inverted spectra, vary from 1 to 100.

After obtaining model parameters from the above inversion technique, source parameters such as seismic moment, source radius and stress drop are estimated using following empirical equations:

$$\textbf{Seismic Moment } (M_0) = \frac{4\pi\rho\beta^3 R \sqrt{(\Pi^2_Z + \Pi^2_R + \Pi^2_T)}}{FR_{\theta\phi}} \quad (8)$$

(Brune, 1970)

$$\textbf{Source Radius } (r) = \frac{2.34 * 3 * \beta}{2\pi \sqrt{f_{cZ} + f_{cR} + f_{cT}}} \quad (9)$$

(Madariaga, 1976)

$$\textbf{Stress Drop } (\Delta\sigma) = \frac{M_0\ [(f_{cZ} + f_{cR} + f_{cT})]^3}{3 * 0.49 * \beta} \quad (10)$$

(Keilis-Borok, 1959)

where, Π_i and f_i mark the long-period spectral level (in m-s) and corner frequency (in Hz) for corresponding three component (Z, R, and T) digital seismograms, respectively, and, '*b*' and '*ρ*' are the S-wave velocity in m/s and rock density in kg/m^3 at the source, respectively. Since our source depth is 8 km, we use a P-wave velocity (α) of 6200 m/s and a density (ρ) of 2700 kg/m^3, for the estimation of source parameters. We calculated '*ρ*' from the P-wave velocity using the relation [ρ(gm/cm^3) = 0.32 *V_p(km/s) + 0.77 (Berteusen, 1977)]. P accounts for equal partition of energy in the two horizontal components (= $1/\sqrt{2}$). $R_{\varphi\phi}$ is the mean radiation pattern, which is assumed to be 0.63 here for S-waves (Aki and Richards, 1980). 'F' is the free surface correction factor (=2). The estimated 'M_0', 'r' and stress drop are in 'N-m', 'm', and 'Pa', respectively (1 MPa = 10^6 Pa).

And, $G(R)$, the geometrical factor term, is considered to be as follow:

$$G(R) = \begin{bmatrix} R & \text{for } R \le R_0 \\ \sqrt{RR_0} & \text{for } R > R_0 \end{bmatrix} \quad (11)$$

where, R_o = 100 km. This form of G(R) implies predominance of body waves for R < 100 km and of surface waves beyond this distance. And, G(R) is geometrical spreading factor. Here, $G(R) = \sqrt{RR_o}$ is used

for six stations (i.e. epi. dist. >100 km) according to equation (11) while for the remaining three stations we used G(R)=R, where, 'R' is the hypocentral distance in m.

Moment Tensor Inversion

The moment tensor (MT) inversion for multiple point sources is performed using the ISOLA software (Sokos and Zahradnik, 2008), which uses the iterative deconvolution technique of Kikuchi and Kanamori (1991) for inversion of complete regional and local waveforms (Sokos and Zahradnik, 2013). In this method, first the discrete wave number method of Bouchon (1981) and Coutant (1989) are used to compute the full wavefield synthetics (i.e. Green's functions at local and regional distances), using a set of predefined point-source positions along a line or on a plane. After obtaining a major point-source contribution or sub-event, the corresponding synthetics are subtracted from data. Then, the residual waveform is inverted for another point source, and so on (Zahradnik et al., 2005). Here, the point sources are removed consecutively, one after another, thus, each step involves only two parameters (source position and onset time), which provides stability of the inversion (Zahradnik et al., 2005). To get the best position and onset time, a grid search method is used that provides the best position and time in terms of the absolute value of the correlation coefficient between the observed and synthetics. The correlation coefficients are calculated automatically during least squares inversion (Dimri, 1992; Zahradnik et al., 2005). At the best-fitting spatio-temporal position, the match between the observed and synthetics data is characterized by the overall variance reduction (over all stations and components) (Zahradnik et al., 2005). The remaining part (i. e. the deviatoric moment tensor inversion) is linear, which calculates only five moment tensor components. An L2 norm least squares inversion is used to obtain the moment tensors of the subevents by minimizing the difference between observed and synthetic displacements, whose moment rate has a predefined shape and duration. In our modeling, a delta function is used.

In this paper, the deviatoric moment tensor inversion available in the ISOLA-GUI package was used (Sokos and Zahradnik 2008 and 2013). The constraint is nonlinear, which is applied iteratively using the method of Lagrange multipliers. The details of the technique can be found in Zahradnik et al. (2005). Velocity records in SAC format as input data for moment tensor inversion was used. The data is processed in different steps by using the software like band-passed (here 0.06-0.14 Hz) filtering, cosine tapering (5%), origin alignment etc. ISOLA integrates the input data to the band-passed displacement, which are then used as input for the moment tensor inversion. A four band passed filter (f_1, f_2, f_3, f_4), which is applied both to real and synthetic wave forms, is flat (=1) between f_2 and f_3, and cosine-tapered between f_1 and f_2, and again between f_3 and f_4. The SNR curves help mainly to define f_1, because the noise level (either natural or instrumental) limits the usable low-frequency range (Sokos and Zahradnik, 2013). The f_4 value is dictated by knowledge of the earth structure. With existing crustal models, near stations (<<"100 km) can be inverted up to <"1 Hz, whereas near-regional stations (<"100 km) can be inverted up to <"0.1 Hz, and regional stations <"1000 km up to <"0.01 Hz (Sokos and Zahradnik, 2013). In this paper, station dependent frequency range is used according to the SN (signal-to-noise) ratio and the epicentral distance. Here, frequency range (0.06 0.08 0.12 0.14) for the moment tensor inversion was used.

RESULTS

The estimated source parameters of the 15 December 2015 Deogarh event at two broadband stations are listed in Table 2, which are estimated by inverting the S-wave displacement spectra from the three-component (RTZ) recordings, wherein, an iterative Levenberg-Marquardt inversion technique is used. Here, a range of the adjustable damping parameter (ë) varying from 1 to 100 to obtain the best fitting S-wave spectra through the Levenberg–Marquardt inversion was used. The estimated S-wave spectra for the R, T and Z components for two broadband seismograph stations in the eastern Indian shield are shown in Figs. 3a-f, which show very stable nature of the S wave spectra clearly defining the long-period spectral level (P_o) and corner frequency (f_c). The ln(P_o) and f_c obtained from the best fit spectra, which is determined through the Levenberg–Marquardt inversion of the S-wave spectra, are also shown in Figs. 3a-f. In this study, the sampling rate of broadband data is 50 sps. Thus, the maximum frequency content of spectra is defined by the Nyquist frequency (sps/2), i.e., 25 Hz. The estimated seismic moment (M_o) and source radius (r) vary from 8.8 x 10^{14} (at CHI) to 1.3 x 10^{15} N-m (at RAM) and 180.8 m (at CHI) to 180.4 m (at RAM), respectively, while estimated stress drops ("ó) range from 11.70 (at CHI) to 16.84 MPa (at RAM), respectively (Table 1). The corner frequencies (f_c) are found to range from 4.06 (at CHI) to 4.07 Hz (at RAM) while moment magnitudes vary from 3.9 (at CHI) to 4.1 (at RAM) (Table 1). The mean f_c, r, M_o, Ds, and M_w for the 15 December 2015 event are found to be 4.1 Hz, 180.6 m, 1.1 x 10^{15} N-m, 14.27 MPa, and 4.0, respectively.

Table 2. Estimated source parameters of the 15 December 2015 Deogarh event

Station	Cor. Freq., f_c in Hz	M_o in N-m	Sou. Rad., r in m	$\Delta\sigma$ in MPa	M_w
RAM	4.06	8.80E+14	180.80	11.70	3.90
CHI	4.07	1.30E+15	180.30	16.84	4.10

The 15 December 2015 main shock occurred at the location of latitude 24.034ºN, longitude 86.649ºE. For the multiple source moment tensor inversion of this event, three-component broadband waveforms from four broadband stations (NRS, RAM, DMK, and HAZ) are used

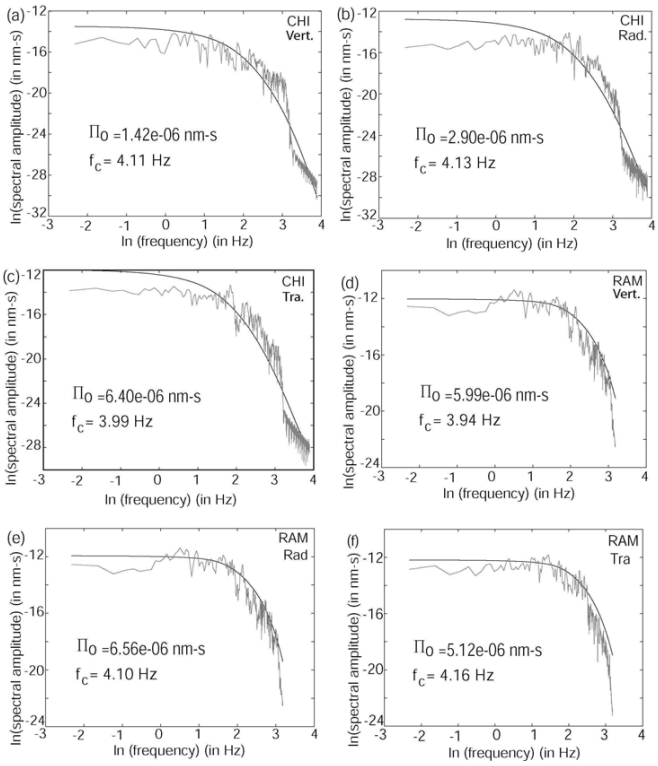

Fig.3. Spectral modeling of S-wave spectra for three component RTZ data for two seismograph stations (**a-c**) CHI, (**d-f**) and RAM. Estimated corner frequency, f_c and ln (long-period spectral level, $\prod_o$) obtained from inversion modeling of S-wave spectra for each station are also shown.

(Fig. 4). The epicentral distances for NRS, RAM, DMK, and HAZ are 19.4, 36.0, 76.2, and 129.0, respectively. The displacement traces for the remaining five far stations (CHI, SAL, BLS, BHN, and KHU) are found to be oscillatory and noisy, due to their large epicentral distances of 195-438 km (Table 1). Therefore, the data from these stations are not used in the MT inversion. A four band-passed filter (0.06, 0.08, 0.12, 0.14 Hz) is used for the MT inversion. The deviatoric constrained full waveform moment tensor inversion for multiple point-sources (source below the epicenter) is performed, using ISOLA software, on the band-passed (0.06-0.14 Hz) displacement traces of the 2015 event obtained from the five broadband stations of the seismic network of CSIR-NGRI, Hyderabad (Fig. 1). The good agreement between observed traces and synthetics are shown in Fig.4. For the deviatoric constrained full waveform MT inversion for multiple sources below the epicenter, we consider a set of predefined 10 point-source positions at every 3 km depth beneath the mainshock epicenter starting from 2 to 45 km. The inversion provides the maximum spatial correlation at 8 km depth for the 3rd source position (Fig. 5a), suggesting a solution having 70% of double-couple (DC) component and 30% of compensated linear vector dipole (CLVD) component (Fig. 5c). The best-fit mechanism at 8 km centroid depth suggests a right-lateral strike slip mechanism, with the strike, dip, and rake of 167°, 72° and 169°, respectively (Fig. 5b). The seismic moment and moment magnitude are estimated to be 5.0 x 10^{14} N-m and 3.7, respectively. The P-axis orientation is estimated to be N24°E for this event indicating the maximum compression acting in the NE direction in the lower crust, underlying the CGGT, which agrees with the absolute plate motion of the Indian plate (Fig. 1).

DISCUSSION AND CONCLUSION

In this paper, source parameters and moment tensor solution of the 15 December 2015 Deogarh event through inversion modelling of broadband data from a seismic network of 15 three-component seismographs deployed in the eastern Indian craton was estimated. The average seismic moment and source radius for the 21 May 2015 event is estimated to be 1.1 x 10^{15} N-m and 180.6 meters, respectively, while average stress drop and corner frequency are found to be 14.27 MPa and 4.1 Hz, respectively. The estimated high-stress drop of 14.27

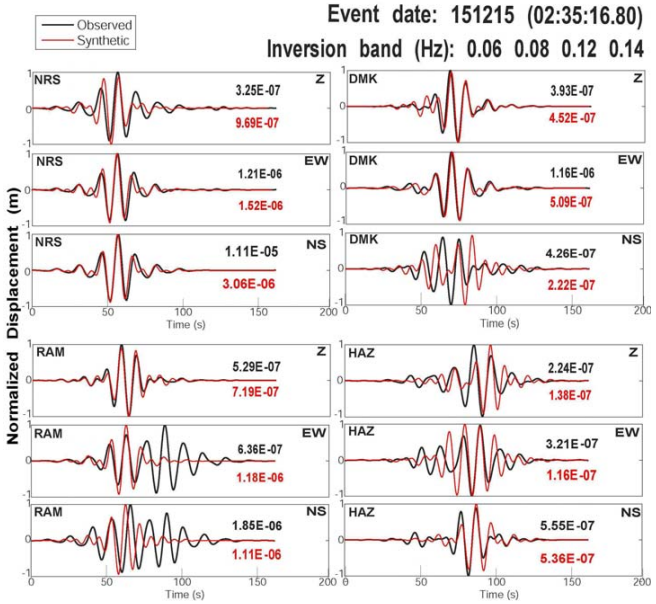

Fig.4. Solutions of deviatoric constrained full wave-filed MT inversion for the 15 December 2015 Deogarh event for multiple point sources below the epicenter, showing Synthetic (red lines) and observed (black lines) traces.

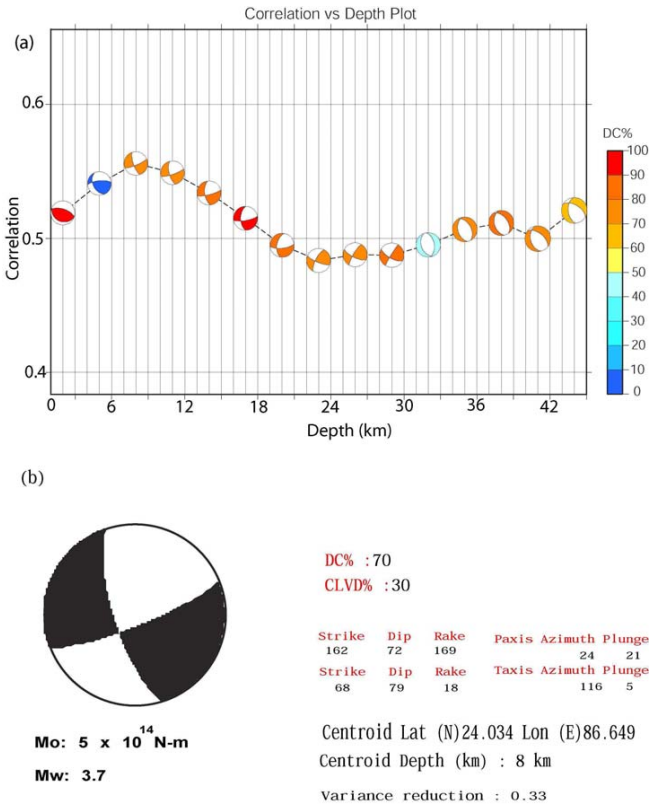

Fig.5. Solutions of deviatoric constrained moment tensor (MT) inversion for the 2015 Deogarh event for multiple point sources below the epicenter (a) A plot showing correlation with source depth, and (b) A plot showing focal mechanism for the best fit solution showing maximum correlation with source depth.

MPa for the M_w4.0 Deogarh event, which is comparatively higher than the existing stress drop estimates of similar size earthquakes from other intraplate regions of the Indian sub-continent. This high-stress drop could be attributed to the strike-slip nature of this earthquake. The strike-slip fault in the mafic upper crust can accumulate large stresses, which, in turn, can result in large stress drops.

The location of the 2015 Deogarh event lies in the Damodar Graben of Gondwana age, where the existing focal mechanism solutions of earthquakes during last few decades show a dominant strike-slip regime with almost NE trending P-axes. The deformation data suggests that the Indian subcontinent is moving northward at a rate of approximately 52 to 63 mm/yr, and is colliding with the northward moving Asian plate (Burgmann et al., 2001). The forces related to this collision apparently control the current pattern of tectonic activity in India, which led to the domination of NNE-NE compression over the Indian plate. Modeling of intraplate stresses and GPS studies for Indian region showed a dominant NE compression over the Indian plate resulted from the northward movement of the Indian plate (Cloetingh and Wortel, 1986; Coblentz et al.,1998; Bilham, 1999; Paul et al., 2001). Small to moderate size earthquakes have been occurring in CGGT (Gupta et al., 2014). Until today, the region has experienced two historical damaging earthquakes (viz.31 July 1868 M4.3 Hazaribagh and 30 September 1868 M5.7 Manbhum (Oldham, 1883). The left lateral strike-slip faulting has been shown to be the dominant deformation mode for the region through the moment tensor solutions of two local earthquakes of M<3.0, which occurred in the surrounding regions of Dhanbad, Jharkhand (Fig. 1; Kayal et al., 2009).

In accordance with the above-mentioned seismological observations, the estimated source mechanism obtained by the iterative

inversion of nine station broadband data of the 15 December 2015 Deogarh event revealed a right-lateral strike-slip motion at 8 km centroid depth below the study area. The P-axis orients toward N24ºE that corroborates well with the absolute plate motion of Indian plate as predicted by the NUVEL1A model (Demets et al., 1990). While the T-axis orients toward EW direction, which aligns well with the strike of Damodar graben (DG) of Gondwana age. The faults/fractures within DG are neotectonically active, which has reactivated to generate small to moderate size earthquakes in the past. Thus, we propose that the Deogarh earthquake is generated by the neotectonic reactivation of a fault associated with DG. The cause of fault reactivation could be attributed to the occurrence of low friction material (Morrow et al., 1992) or the presence of high fluid pressure in the fault zone (Byerlee, 1978; Sibson, 1984). The short period of instrumental monitoring, poorly known seismicity, and lack of systematic geophysical investigations in the Eastern Indian shield indicate that further studies are necessary to address this problem.

Acknowledgements: Authors are grateful to the Director, NGRI, Hyderabad, for his kind permission to publish this work. This study is supported by the Council of Scientific and Industrial Research (CSIR) twelfth five year plan project (Index) at the CSIR-National Geophysical Research Institute, Hyderabad.

References

Berteusen, K.A. (1977) Moho depth determinations based on spectral ratio analysis of NORSAR long-period P waves. Phys. of Earth and Planet Int., v.31, pp.313-326.

Bilham, R. (1999) Slip parameters for the Rann of Kachchh, India, 16 June 1819 earthquake quantified from contemporary accounts. *In:* Stewart, I.S., Vita-Finzi, C. (Eds.), Coastal Tectonics, 146. Geol. Soc. London, pp. 295–318.

Boatwright, J. (1980) A spectral theory for circular seismic sources: simple estimates of source dimension, dynamic stress drop and radiated energy. Bull. Seism. Soc. Amer., v.70, pp. 1-27.

Bouchon, M. (1981) A simple method to calculate Green's functions for elastic layered media. Bull. Seismol. Soc. Amer., v.71, pp. 959–971.

Brune, J. N. (1970) Tectonic stress and the spectra of seismic shear waves from earthquakes. Jour. Geophys. Res., v.75, pp. 4997–5009.

Burgmann, P.J., Gaur, V.K., Bilham, R., Larson, K.N., Ananda, M.B., Jade, S., Mukul, M., Anupama, T.S., Satyal, G. and Kumar, D. (2001) The motion and active deformation of India. Geophys. Res. Lett., v.28 (4), pp.28–32.

Byerlee, J. (1978) Friction of rocks. Pure Appld. Geophys., v.116, pp.615-626.

Chandra, U. (1977) Earthquakes of Peninsular India - a seismotectonic study. Bull. Seismol. Soc. Amer., v.67(5), pp.1387-1413.

Cloetingh, S.A.P.L. and Wortel, M.J.R. (1986) Stresses in the Indo-Australian plate. Tectonophysics, v.132, pp.49–67.

Coblentz, D.D., Zhou, S., Hillis, R.H., Richardson, R.M. and Sandiford, M. (1998) Topography, boundary forces, and the Indo-Australian intraplate stress field. Jour. Geophys. Res., v.103, pp.919–931.

Coutant, O. (1989) Program of numerical simulation AXITRA; Research Report, Laboratoire de Ge´ophysique Interne et Tectonophysique, Grenoble.

DeMets, C., Gordon, R.G., Argus, D.F. and Stein, S. (1990) Current plate motions. Geophys. Jour. Internat., v.101, pp.425–478

Dimri, V.P. (1992) Deconvolution and Inverse Theory: Application to Geophysical Problems. Elsevier Science Publishers, Amsterdam, 230p.

Fletcher, J.B. (1995) Source parameters and crustal Q for four earthquakes in South Carolina, Seismol. Res. Lett., v.66, pp.44–58.

Gupta, S., Mohanty, W. K., Mandal, A. and Misra, S. (2014) Ancient terrane boundaries as probable seismic hazards: A case study from the northern boundary of the Eastern Ghats Belt, India. Geoscience Frontiers, v.5, pp.17-24.

Havskov, J. and Ottemoller, L. (2003) SEISAN: the earthquake analysis software manual, p. 203.

Kayal, J.R., Srivastava, V.K., Bhattacharya, S.N., Khan, P.K. and Chatterjee, R. (2009) Source Parameters and Focal Mechanisms of Local Earthquakes: Single Broadband Observatory at ISM Dhanbad. Jour. Geol. Soc. India, v.74, pp.413-419.

Keilis-Borok, V. I. (1959) An estimation of the displacement in earthquake source and of source dimensions. Ann. Geophys., v.12, pp.205–214.

Kennett, B. L. N. and Engdahl, E.R. (1991) Travel times for global earthquake location and phase identification. Geophys. Jour. Internat., v.105, pp.429–465, doi 10.1111/j.1365-246X.1991.tb06724.x.

Khan, P.K., Biswas, B., Samdarshi, P. and Prasad, R. (2011) Seismicity and the coda-Q variation in eastern Indian shield region. Indian Jour. Geosci., v.65(2), pp.43–50.

Mandal, P. and Dutta, U. (2011) Estimation of earthquake source parameters and site response. Bull. Seismol. Soc. Amer., v.101(4), pp.1719–1731.

Madriaga, R. (1976) Dynamics of an expanding circular fault. Bull. Seismol. Soc. Amer., v.66, pp.639–666.

Morrow, C., Radney, B. and Byerlee, J. D. (1992) Frictional strength and the effective pressure law of montmorillonite and illite clays: fault mechanics and transport properties of rocks; In Fault Mechanics and Transport Properties of Rocks. ed. Evans B and Wong T F San Diego, California: Academic Press, pp.69–88.

Oldham, T. (1883) A catalogue of Indian earthquakes from the earliest times to the end of 1869 A.D.. Mem. Geol. Surv. India., v.XIX, Part. 3.

Paul, J., Burgmann, R., Gaur, V.K., Bilham, R., Larson, K.M., Ananda, M.B., Jade, S., Mukul, M., Anupama, T.S., Satyal, G. and Kumar, D. (2001) The motion and active deformation of India. Geophys. Res. Lett., v.28, pp.647–651.

Press, W. H. et al. (1992) Numerical recipes in FORTRAN and C. Academic Press New York, pp.382.

Seismic Analysis Code (SAC2000) (2000) (http://www.iris.edu/manuals/sac/SAC_Home_Main.html)280.

Sibson, R.H. (1984) Roughness at the base of the seismogenic zone: contributing factors. Jour. Geophys. Res., v.89, pp.5791-5799.

Singh, S. K., Garcý´a, D., Pacheco, J. F., Valenzuela, R., Bansal, B. K. and Dattatrayam, R. S. (2004) Q of the Indian Shield. Bull. Seismol. Soc. Amer., v.94(4), pp.1564–1570.

Sokos, E.N. and Zahradník, J. (2008) ISOLA a FORTRAN code and a MATLAB GUI to perform multiple-point source inversion of seismic data; Comput. Geosci., v.34, pp.967–977.

Sokos, E.N. and Zahradník, J. (2013) Evaluating Centroid-Moment-Tensor uncertainty in the new version of ISOLA software. Seismol. Res. Lett., v.84(4), pp.656-665.

Zahradnik, J., Serpetsidaki, A., Sokos, E. and Tselentis, G. A. (2005) Iterative deconvolution of regional waveforms and a double-event interpretation of the 2003 Lefkada Earthquake, Greece. Bull. Seismol. Soc. Amer., v.95(1), pp.159–172.

(Received: 5 January 2016; Revised form accepted: 14 July 2016)